Proceedings of the 17th World Congress
The International Federation of Automatic Control
Seoul, Korea, July 6-11, 2008

Sensor Fault Diagnosis of Wind Turbines for Fault Tolerant ⋆

X. Wei * **M. Verhaegen** ** **T. van den Engelen** ***

* *Delft Center for Systems and Control, Delft University of Technology, Delft, Mekelweg 2, 2628 CD, The Netherlands.(e-mail: xiukun.wei@tudelft.nl.)*
** *Delft Center for Systems and Control, Delft University of Technology, Delft, Mekelweg 2, 2628 CD, The Netherlands.(e-mail: m.verhaegen@moesp.org)*
*** *The wind energy department,the Energy Research Center of the Netherlands. (e-mail: vanengelen@ecn.nl)*

Abstract: This paper aims at the blade root moment sensor fault detection and isolation issue. The underlying problem is crucial to the successful application of the individual pitch control system which plays a key role for reducing the blade loads of large offshore wind turbines. In this paper, a wind turbine model is built based on the closed loop identification technique, where the wind dynamics is included in the model. The fault detection issue are investigated based on the residual generated by Kalman filter. The additive faults and multiplicative faults are investigated respectively. For the additive fault case, the mean value change detection of the residual and the generalized likelihood ratio test are utilized respectively. On the other hand, the multiplicative fault is handled by the variance change detection of the residuals. The fault isolation issue is proceeded with the help of dual sensor redundancy. Simulation results show that the proposed approach can be successfully applied to the underlying issue.

1. INTRODUCTION

Wind energy has been received much more attention than ever before in the last decade. It will play a more and more important role in the future energy market since the decreasing production of the fossil energy, mainly from oil, which will be almost totally exhausted in the next five or six decades. However, wind energy can not compete with traditional energies up until now since it is more expensive than others. Even though the availability can be up to 98% for onshore wind turbines, the cost due to maintenance are still very high. For offshore wind power systems the availability may fall below 60% due to the downtime of the wind turbines, which is mainly caused by the failures of some components of wind turbines. Therefore, much effort is needed to enhance the reliability of the wind turbines.

This paper aims at the blade root moment sensor faults detection issue, where the sensors are mainly utilized for the blade loads reduction based on individual pitch control strategies (van Engelen and van der Hooft 2003), especially for large scale offshore wind turbines. In wind turbines, strain gauge sensors are nowadays more often used than other types of moment sensors, such as piezoelectric sensors. However, the lifetime of strain gauge is normally not very long compared with that of the other sensors in wind turbine systems. There are several reasons which cause higher failure rates. The strain in the blades is rather high, which has effect on the gauges themselves as well as on the bonding. The harsh environment factors, such as lightning, salty spray, moisture and corrosion, can have direct effects on the bonding and wiring. In addition, the sensors can be easily damaged by maintenance people. The failure rate can be around one failure per year. For wind turbines with three blades, the failure rate is 3 failures per year. This is not desired for offshore wind turbine systems since the sensor failures lead to wrong control behavior of the individual pitch control system, which is crucial for blades loads reduction to prolong the wind turbine lifetime. Therefore, the sensor fault detection of the rotor blades moments is extremely important for successful individual pitch control application. Meanwhile, dual sensor redundancy (two blade root moment sensors are installed at each blade root) is utilized for fault tolerant purpose. In the light of the sensor fault detection alarms, a new sensor set, which are in good condition, can be configured in order to send proper measured signals to the control systems.

To achieve our sensor fault isolation goal, in this paper, two parallel fault detection procedures are utilized at the same time. On the one hand, the output signals of each sensor pair (at the same blade root) are compared directly. The difference is monitored by mean change detection or variance change detection. Which sensor pair has fault can be detected in this step. However, we can not identify which sensor has fault. On the other hand, model based fault detection is applied to monitor the changes of the three sensors (sensor set 1), which are being used by the individual pitch control system, and the rest sensors (sensor set 2), which are redundant sensors. In this procedure, which sensor set has fault can be detected. The fault isolation issue can be done by logic reasoning based on the two procedures.

The remainder of this paper is organized as follows. In the second section, the wind turbine system is briefly introduced. The closed-loop system identification and residual generator based on Kalman filter are presented in the third section. Fault detection techniques, mainly the mean value change, variance change detection, the generalized likelihood techniques and fault isolation with the help of dual sensor redundancy, are

⋆ This work is supported by SenterNovem, an agency of the Dutch Ministry of Economic Affairs, in the projected Sustainable Control, a New Approach to Operate Wind Turbines (SUSCON), under grant EOSLT02013.

reported in the fourth section. In the fifth section, the simulation results are shown to illustrate the effectiveness of the proposed sensor fault diagnosis approach. Some conclusions close this paper.

2. WIND TURBINE SYSTEM AND PROBLEM STATEMENT

2.1 Wind Turbine Plant Model

Define system states, disturbances, inputs and outputs as follows:

$$x = (\ \Omega_r\ \ x_{fa}\ \ \dot{x}_{fa}\ \ x_{sd}\ \ \dot{x}_{sd}\ \ \gamma\ \ \dot{\gamma}\ )^T \tag{1}$$
$$d = (\ v_1\ \ v_2\ \ v_3\ )^T \tag{2}$$
$$u = (\ \theta_1\ \ \theta_2\ \ \theta_3\ \ \delta T_g\ )^T \tag{3}$$
$$y = (\ \Omega_g\ \ \dot{x}_{fa}\ \ \dot{x}_{sd}\ \ \delta M_{z1}\ \ \delta M_{z2}\ \ \delta M_{z3}\ )^T \tag{4}$$

The system state space description then becomes

$$\dot{x} = Ax + B_1(\psi)d + B_2(\psi)u \tag{5}$$
$$y = C(\psi)x + D_1 d + D_2 u \tag{6}$$

where ψ is the blade azimuth angle which is measurable online. Due to the space limitation, the detailed equations are not listed here. Please refer to (van Engelen 2006) for the details.

The underlying system is time varying since the parameters depend on the azimuth ψ. It is a time varying system. However,by Coleman transformation, it can be transferred into a linear time invariant system.

2.2 Linear Time Invariant Model in the Coleman Domain

Coleman transformation is widely adopted to analysis three blades wind turbine systems, which transfer the underlying system from a rotational coordinate to a fixed coordinate system where all periodic coefficients vanish and are replaced by modulation requirements on the input and output signals. Since the simplified wind turbine model does not contain non-coaxial state variables on the shaft or blades, the Coleman-transformation of state variables does not apply.

The Coleman transformation can be described as

$$P = \begin{pmatrix} 1 & sin(\psi_1) & cos(\psi_1) \\ 1 & sin(\psi_2) & cos(\psi_2) \\ 1 & sin(\psi_3) & cos(\psi_3) \end{pmatrix} \tag{7}$$

$$P^{-1} = \begin{pmatrix} \frac{1}{3} & \frac{1}{3} & \frac{1}{3} \\ \frac{2}{3}sin(\psi_1) & \frac{2}{3}sin(\psi_2) & \frac{2}{3}sin(\psi_3) \\ \frac{2}{3}cos(\psi_1) & \frac{2}{3}cos(\psi_2) & \frac{2}{3}cos(\psi_3) \end{pmatrix} \tag{8}$$

$$(\ \theta_1\ \ \theta_2\ \ \theta_3\ )^T = P\,(\ \theta_{cm1}\ \ \theta_{cm2}\ \ \theta_{cm3}\ )^T \tag{9}$$
$$(\ v_1\ \ v_2\ \ v_3\ )^T = P\,(\ v_{cm1}\ \ v_{cm2}\ \ v_{cm3}\ )^T \tag{10}$$
$$(\ M_{cm1}\ \ M_{cm2}\ \ M_{cm3}\ )^T = P^{-1}\,(\ M_{z1}\ \ M_{z2}\ \ M_{z3}\ )^T \tag{11}$$

Define system states, disturbances, inputs and outputs as follows:

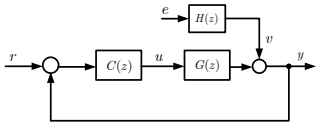

Fig. 1. The wind turbine feedback system

$$x = (\ \Omega_r\ \ x_{fa}\ \ \dot{x}_{fa}\ \ x_{sd}\ \ \dot{x}_{sd}\ \ \gamma\ \ \dot{\gamma}\ )^T \tag{12}$$
$$d_{cm} = (\ v_{cm1}\ \ v_{cm2}\ \ v_{cm3}\ )^T \tag{13}$$
$$u_{cm} = (\ \theta_{cm1}\ \ \theta_{cm2}\ \ \theta_{cm3}\ \ \delta T_g\ )^T \tag{14}$$
$$y_{cm} = (\ \Omega_g\ \ \dot{x}_{fa}\ \ \dot{x}_{sd}\ \ \delta M_{zcm1}\ \ \delta M_{zcm2}\ \ \delta M_{zcm3}\ )^T \tag{15}$$

The system state space description

$$\dot{x} = A_{cm}x + B_{cm1}d_{cm} + B_{cm2}u_{cm} \tag{16}$$
$$y_{cm} = C_{cm}x + D_{cm1}d_{cm} + D_{cm2}u_{cm} \tag{17}$$

Further detailed modeling procedure can be found in (van Engelen 2006).

3. CLOSED-LOOP IDENTIFICATION AND RESIDUAL GENERATOR

3.1 Plant Modeling via Closed-loop Identification

Closed loop identification is necessary for our purpose, because the open loop system is unstable and the system parameters are probably not precise enough. Besides that we want to build a model for wind speed. The controlled wind turbine system can be simplified as the structure shown in Fig. 1, where v represents the wind speed on the output signal and it is modeled by a linear system driven ($H(z)$) by a white noise e. Internal signals in the system represented by $H(z)$ then correspond to the (Coleman transformed) blade effective wind speeds in equation (13). Since we only consider the fault detection issue of the three blade root moments in this paper, the other outputs $\{\Omega_r, \dot{x}_{fa}, \dot{x}_{sd}\}$ are not included in the model afterwards.

The plant in Coleman domain can be parameterized in an innovation form as the following:

$$x_{k+1} = \overline{A}x_k + \overline{B}u_k^{cm} + Ke_k \tag{18}$$
$$y_k^{cm} = \overline{C}x_k + \overline{D}u_k^{cm} + e_k \tag{19}$$

The identification issue now is to determine the system matrix set $\{\overline{A}, \overline{B}, \overline{C}, \overline{D}, K\}$. The advantage of using this model structure is that the gain K can be directly utilized as the steady Kalman filter gain. For more detailed explanation on this model and its relation, please refer to our book (Verhaegen and Verdult 2007). The method adopted in this work is the one described in (Chiuso 2007). The identified model has a $20th$ order. Validation results show that the identified model have satisfied precision.

3.2 Residual Generation Based on Kalman Filter

Based on the identified model of the wind turbine in the Coleman domain, the residual generator for sensor fault detection purpose is shown in Fig. 2, where **CT** and **ICT** represent the Coleman transformation and inverse Coleman transformation respectively. K is the controller. The sensor faults, f_1 and f_2, can be additive faults or multiplicative sensor faults. It is worth

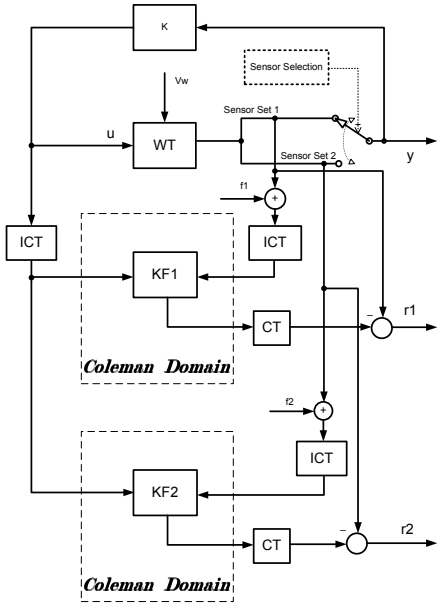

Fig. 2. Dual Kalman Filter Fault Detection Scheme

to notice that the sensor faults have different expressions in the original domain (before the variables are transformed into Coleman domain) and in the Coleman domain. This will be analyzed in the next section in details.

Meanwhile, two kalman filters (**KF1** and **KF2**)are utilized to generate innovations (**r1** and **r2**) for fault detection corresponding to the sensor sets (each set has three sensors) as shown in Fig. 2.

4. FAULT MODELING AND DETECTION

4.1 Fault Modeling

The fault considered in this paper are the additive fault, multiplicative faults, sensor output stuck on a fixed value and slow drifting fault and we assume that only one sensor fault appear each time.

- Additive fault $M_{zi}^f = M_{zi} + \Delta M_{zi}$
- Multiplicative fault $M_{zi}^f = \delta M_{zi}$, where $0 \leq \delta \leq \infty$
- Output stuck $M_{zi}^f = C_o$, C_o is a constant.
- Slow drifting $M_{zi}^f = M_{zi} + \alpha t$

where $i = 1, 2, 3$, α is a small variation rate and t is the time.

With inverse Coleman transformation, one sensor fault results in the variation of all the virtual moments $M_{cm1}, M_{cm2}, M_{cm3}$ in the Coleman domain.

$$\begin{pmatrix} M_{cm1}^f \\ M_{cm2}^f \\ M_{cm3}^f \end{pmatrix} = \begin{pmatrix} M_{cm1} + \frac{1}{3}\Delta M_{zi} \\ M_{cm2} + \frac{2}{3}\sin(\psi_i)\Delta M_{zi} \\ M_{cm3} + \frac{2}{3}\cos(\psi_i)\Delta M_{zi} \end{pmatrix}$$

where $i = 1, 2, 3$.

4.2 Residual without sensor faulty

The identified model (discrete) with an innovation form can be described as

$$x_{k+1} = \widetilde{A}x_k + \widetilde{B}u_k^{cm} + KP_k^{-1}y_k \tag{20}$$
$$y_k^{cm} = \widetilde{C}x_k + \widetilde{D}u_k^{cm} + e_k \tag{21}$$
$$y_k = P_k\widetilde{C}x_k + P_k\widetilde{D}u_k^{cm} + P_k e_k \tag{22}$$

where $\widetilde{A} = \overline{A} - K\overline{C}$, $\widetilde{B} = \overline{B} - K\overline{D}$, $\widetilde{C} = \overline{C}$, $\widetilde{D} = \overline{D}$. $\widetilde{A}$ has eigenvalues in the unit disc (Verhaegen and Verdult 2007, Mangoubi 1998).

The Kalman filter can be expressed as:

$$\widehat{x}_{k+1} = \widetilde{A}\widehat{x}_k + \widetilde{B}u_k^{cm} + KP_k^{-1}y_k \tag{23}$$
$$\widehat{y}_k^{cm} = \widetilde{C}\widehat{x}_k + \widetilde{D}u_k^{cm} \tag{24}$$
$$r_k = P_k\widetilde{C}\varepsilon_k + P_k e_k \tag{25}$$

where $\varepsilon_k = x_k - \widehat{x}_k$, $\varepsilon_k \sim (0, \sigma_\varepsilon)$, e_k is a white noise sequence and its mean value $E\{e_k\} = 0$ and its covariance $covar(e_k) = \sigma I$.

4.3 Additive Fault Detection Based on Residual Mean Value

When the sensor has additive faults, the sensor output is

$$y_k^f = y_k + V^i f_{k-\tau^*}^s \tag{26}$$

where $V^i, i = 1, 2, 3$ describes the sensor faulty direction. Here we define $V^1 = (1\ 0\ 0)'$, $V^2 = (0\ 1\ 0)'$ and $V^3 = (0\ 0\ 1)'$ represents that faults from three senors respectively. $f = Vf_{k-\tau^*}^s$ is the sensor fault. τ^* is the time that the sensor fault appear.

The output of the Kalman filter is

$$\widehat{x}_{k+1}^f = \widetilde{A}\widehat{x}_k^f + \widetilde{B}u_k^{cm} + KP_k^{-1}y_k^f \tag{27}$$
$$\widehat{y}_k^{f,cm} = \widetilde{C}\widehat{x}_k^f + \widetilde{D}u_k^{cm} \tag{28}$$
$$\widehat{y}_k^f = P_k\widetilde{C}\widehat{x}_k^f + P_k\widetilde{D}u_k^{cm} \tag{29}$$

Thanks to the linearity of the system, the states of Kalman filter can be split into two parts which are excited by the system real output y_k and $V^i f_{k-\tau^*}^s$ respectively. That is:

$$y_k^f = y_k + f$$
$$\widehat{x}_k^f = \widehat{x}_k - \xi_k$$
$$\widehat{\varepsilon}_k^f = \widehat{\varepsilon}_k + \xi_k$$
$$\widehat{y}_k^f = \widehat{y}_k + g_{k-\tau^*}\nu$$

the residual with sensor additive faults is

$$r_k^f = r_k + g_{k-\tau^*}\nu$$

where ν is the magnitude of the fault, r is the residual part while system has no sensor faulty case, g is generated by the following *failure signature equations*:

$$\xi_{k+1} = \widetilde{A}\xi_k - KP_k^{-1}V^i s_{k-\tau^*}^s \tag{30}$$
$$g_{k-\tau^*}^{cm,i} = \widetilde{C}\xi_k + P_k^{-1}V^i s_{k-\tau^*}^s \tag{31}$$
$$g_{k-\tau^*}^i = P_k\widetilde{C}\xi_k + V^i s_{k-\tau^*}^s \tag{32}$$

where s is a unit step signal, $i = 1, 2, 3$

In the absence of fault case, the residual g_k is zero. But in the presence of sensor faults, the residual will not be zero. Monitoring the mean value change, we can directly identify which sensor has fault combining the direct comparison difference of dual sensors.

Stop Ruling for Mean Value Detection The algorithm as follows in (Gustafsson 2000) is utilized for the mean value change detection of signal ζ_k.

Algorithm (CUSUM LS Filter)4.1

$$\begin{aligned}\widehat{\vartheta} &= \frac{1}{t-t_0}\sum_{k=t_0+1}^{t}\zeta_k \\ \varepsilon_{k,i} &= \zeta_k - \widehat{\vartheta} \\ s_k^1 &= \varepsilon_k \\ s_k^2 &= -\varepsilon_k \\ g_k^1 &= max(g_{k-1}^1 + s_k^1 - \nu, 0) \\ g_k^2 &= max(g_{k-1}^2 + s_k^2 - \nu, 0)\end{aligned}$$

Alarm if $g_k^1 > h$ or $g_k^2 > h$. After alarm, reset $g_k^1 = 0$, $g_k^2 = 0$. Parameter ν and h need to be designed. ν is used to prevent positive drifting of the mean value and it can be chosen as one half of the expected change magnitude. The robustness and decreased false alarm rate can be achieved by requiring several $g_k^1 > h$ or $g_k^2 > h$ (Gustafsson 2000).

The estimate $\widehat{\vartheta}$ is the bias between the two sensors at the same blade root. An almost constant output means that one sensor has bias fault. If the estimate is slowly drifting, it is corresponding to the sensor slowly drifting fault. While the estimate is proportional to the filtered output of one sensor, the gain of one sensor is changed. For sensor output stuck case, one sensor has an constant output.

The method presented here can be used for any additive fault. But it takes time to send an alarm after the fault appears.

4.4 Abrupt jump fault detection based on generalized likelihood ratio test (GLRT)

For abrupt jump fault case, it can also be detected by **GLRT** presented in (Gustafsson 2000) where hypotheses test is used.

The hypotheses test can be expressed in terms of the innovation

$$H_0 : \varrho_k = r_k \tag{33}$$

$$H_1 : \varrho_k = r_k + g_k^i(\tau^*)\nu \tag{34}$$

where r_k is the residual in the absence of sensor normal case. $g_k(\tau^*)\nu$ is the part generated by the sensor fault with magnitude ν at time τ^*. g_k is generated by the failure signature dynamical equation. The primary principle behind is that for each time instant k, check if there is a failure in the past time with generalized likelihood ratio

$$\Lambda_k^i(\tau^*,\nu) = \frac{p(\varrho_{k-L},\varrho_{k-L+1},...,\varrho_k|H_1,\tau^*,V^i,\nu)}{p(\varrho_{k-L},\varrho_{k-L+1},...,\varrho_k|H_0)} \tag{35}$$

$$= \prod_{j=k-L}^{j=k}\frac{p(\varrho_j|H_j,\tau^*,V^i,\nu)}{p(\varrho_j|H_0)} \tag{36}$$

Taking the log of the above ratio,

$$\lambda_k^i(\tau^*,\nu) = \mathbf{log}\Lambda_k(\tau^*,V^i,\nu) \tag{37}$$

$$= \nu\chi(\tau^*,V^i) - \frac{1}{2}\nu^2 S_k(\tau^*,V^i) \tag{38}$$

where

$$\chi_k(\tau^*,V^i) = \sum_{j=\tau^*}^{k} g_j^{i,'}(\tau^*)R_j^{-1}\varrho_j \tag{39}$$

$$R_j = \overline{C}P_j\overline{C}' + \overline{DD}' \tag{40}$$

$$S_k(\tau^*,V^i) = \sum_{j=\tau^*}^{k} g_j^{i,'}(\tau^*)R_j^{-1}g_j(\tau^*) \tag{41}$$

P_j is the system noise covariance.

The generalized log likelihood ratio is given by

$$\ell_k^i = \max_{\tau^*\in(k-L,k)}\max_{\nu\in R}\lambda_k(\tau^*,\nu,V^i) \tag{42}$$

where $i = 1, 2, 3$. For the detailed algorithm of GLRT, please refer to (Gustafsson 2000).

4.5 Multiplicative Fault Detection Based on Variance Change Detection

The sensor multiplicative faults can be described as

$$y_k^f = \Delta_i y_k \tag{43}$$

The estimated wind turbine model with the innovation form is also used in this case as follows:

$$x_{k+1} = \widetilde{A}x_k + \widetilde{B}u_k^{cm} + KP_k^{-1}y_k \tag{44}$$

$$y_k^{cm} = \widetilde{C}x_k + \widetilde{D}u_k^{cm} + e_k \tag{45}$$

$$y_k = P_k\widetilde{C}x_k + P_k\widetilde{D}u_k^{cm} + P_k e_k \tag{46}$$

the sensor outputs is

$$y_k^f = \Delta_i(P_k\widetilde{C}x_k + P_k\widetilde{D}u_k^{cm} + P_k e_k) \tag{47}$$

where Δ_i is a diagonal matrix with all the elements 1 except that one is δ_i and $0 < \delta_i < +\infty$.

In this case, the residual is

$$r_k^f = P_k\widetilde{C}\varepsilon_k^f + (\Delta_i - I)P_k\widetilde{C}x_k + (\Delta_i - I)P_k\widetilde{D}u_k^{cm} + \Delta_i P_k e_k$$

The residual can be further split into two parts as in the additive sensor fault case. At first, the sensor output is split into two parts $y_k^f = y_k + (\Delta_i - I)y_k$. The dynamics of the Kalman filter can also be split into two parts in which one part is driven by the sensor fault and the other part is the same as the sensor normal case, that is, the dynamics excited by the sensor faulty part is

$$\widehat{\xi}_{k+1} = \widetilde{\xi}\widehat{x}_k + KP_k^{-1}(\Delta_i - I)y_k \tag{48}$$

$$\eta_k^{cm} = \widetilde{C}\widehat{\xi}_k \tag{49}$$

$$\eta_k = P_k\widetilde{C}\widehat{\xi}_k \tag{50}$$

In sensor normal case, the residual is

$$r_k = P_k\widetilde{C}\varepsilon_k + P_k e_k$$

Now we can obtain

$$r_k^f = r_k + \eta_k + (\Delta_i - I)P_k\widetilde{C}x_k + (\Delta_i - I)P_k\widetilde{D}u_k^{cm}$$

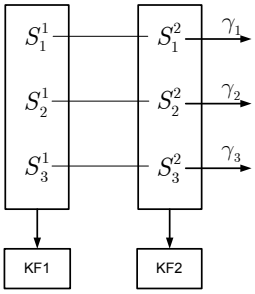

Fig. 3. Dual Sensor Redundancy and Dual Kalman Filters for Sensor Fault Diagnosis Scheme

mean value changes while y_k and/or u_k have DC components, mean value will change.

Variance changes The deterministic part from $(\Delta_i - I)P_k\widetilde{D}u_k$ does not contribute to the residual variance. However, η_k and $(\Delta_i - I)P_k\widetilde{C}x_k$ definitely cause the residual variance change. Based on the variance change detection, it can easily be identified which sensor set has multiplicative fault. But it is not trivial to determine the relation between the faults and the residual. Fortunately, the isolation issue can be done by comparing the outputs of the sensor pairs at each blade root.

Energy Detector for Variance Change Detection The residual variance change detection can simply use the so called ***energy detector*** in (Kay 1998) where the sum of the squared residual in a sliding window is monitored. An alarm is generated if

$$V(r_i) = \sum_{i=k-N+1}^{k} r_i^2 > h$$

where N is the window size and h is the threshold.

4.6 Sensor Fault Isolation Logic and Recombination

Fault Isolation Logic As shown in Fig. 3, there are two set of sensors which send signals to two Kalman filters respectively. The sensors are $S_1^1, S_1^2, \cdots, S_3^1, S_3^2$, where the upper index indicates the first sensor or the second sensor and the lower index indicates the blade. For the two sensors at each blade, they are compared all the time where the output $\gamma_i = S_i^1 - S_i^2$ are the difference between their outputs. Since measured noise, γ_i is not equal to zero even while the sensors are not faulty. However, we can monitor the mean value change or variance change of these residuals to detect the additive faults (sensor output bias, slow drifting and output stuck) and multiplicative faults(sensor gain change) respectively.

Suppose that each time only one set of the sensors can have faults, that is, only one of the innovations r_k^1 or r_k^2 of the two parallel Kalman filters can have change. This indicates in which set the faulty sensors located. In the light of the direct comparison of the dual sensor pairs, the faulty sensors can be isolated. For instance, while the mean values of γ_2 and r_k^1 have changes and r_k^2, γ_1 and γ_3 does not have change, S_2^1 is faulty. If both γ_2 and γ_1 have changes while r_k^1 has change, S_2^1 and S_1^1 are faulty.

Sensor Recombination or Selection As soon as a sensor fault is detected and isolated and the faulty sensor is in the set which is used in the feedback loop, a new set of sensor which are in good condition should be selected to send correct signals to the control system. There are eight possible combinations. The diagnosis result can be recorded for maintenance purpose.

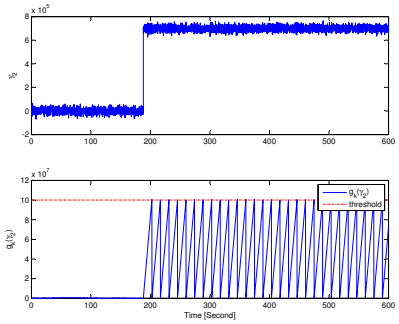

Fig. 4. Upper subplot shows the comparison output γ_2 of the sensors at the second blades. The lower subplot shows the mean value change detection estimate from the CUSUM LS filter, where the dashed line is the threshold.

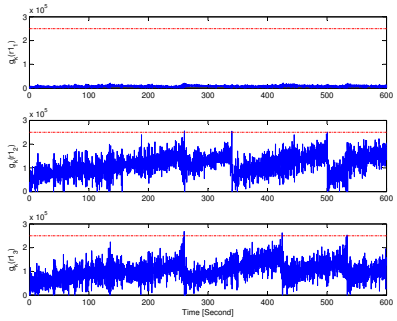

Fig. 5. Mean value change detection results of the three innovation outputs of Kalman filter 1 from the CUSUM LS filter.

5. SIMULATION RESULTS

Fig. 4 shows the output difference of the sensor pair at the second blade and the mean change detection output from the CUSUM LS filter. While the sensor has abrupt jump change since $188s$, the detector begins to alarm repeatedly. The innovation output of Kalman filter 1 (KF1) is also detected that it has mean value change which is shown in Fig. 5, where the thresholds are shown in dashed lines. Fig. 6 shows the results of GLRT while assuming the jump faults are from the three sensors respectively. It can be seen that under all these three hypothesis, the outputs of all the GLRTs have a large peak output after the abrupt jump fault appears. The reason for this phenomena is that the three sensor jump fault has a very similar signature output (see the signature equations.) Based on these detection outputs, we can safely conclude that sensor S_2^1 has a abrupt jump change.

Fig. 7 shows the the comparison output γ_2 of the sensors at the second blades when one of the sensor has slow drifting fault. The lower subplot shows the mean value change detection estimate from the CUSUM LS filter, where the dashed line is the threshold. It can be seen that the alarm frequency is increasing after the slow drifting appears. The innovation mean change detection of Kalman filter 1 are shown in Fig.8. The mean value is changing very slowly. We can conclude that sensor S_2^1 has slow drifting fault.

The sensor S_2^1 gain change detection results based on the energy detector are shown in Fig. 9 and Fig. 10. While the sensor gain is changed to its 1.5 times of its normal gain, the sum

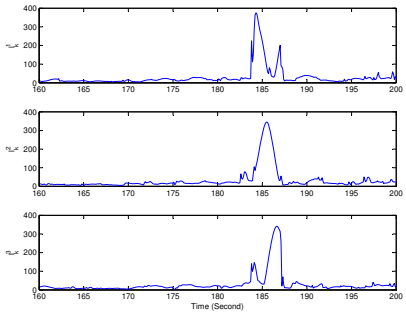

Fig. 6. The top subplot is the GLRT result while assuming sensor S_1^1 has abrupt jump change. The middle one is the GLRT output while assuming S_1^2 has abrupt change. The bottom subplot is the result for assuming that S_1^3 has fault.

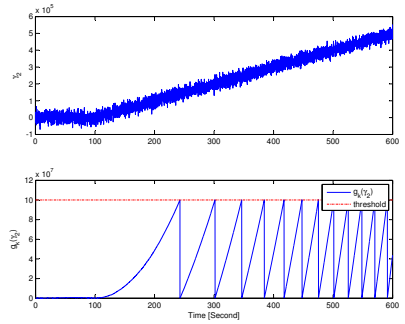

Fig. 7. Upper subplot shows the comparison output γ_2 of the sensors at the second blades while one of the sensor has slow drifting fault. The lower subplot shows the mean value change detection estimate from the CUSUM LS filter, where the dashed line is the threshold.

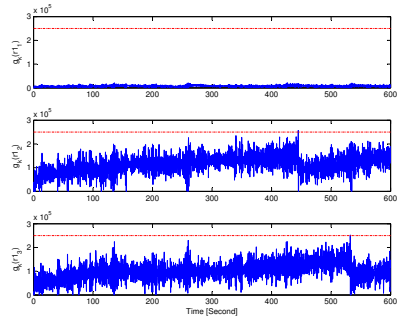

Fig. 8. Mean value change detection results of the three innovation outputs of Kalman filter 1 from the CUSUM LS filter while sensor S_2^1 has slow drifting fault.

of the squared γ_2 has gotten a large change while the fault appears since $300s$. The innovation variance is also detected by the energy detector algorithm. It is not difficult to draw a conclusion that the sensor S_2^1 has multiplicative fault.

6. CONCLUSION

This paper concerns sensor fault detection issue of the rotor blade moments of large scale wind turbine system. The underlying system is extremely important for the load reduction of wind turbines based on the individual pitch control system. Simulation results show that the proposed methods are suitable for the underlying sensor fault detection issue.

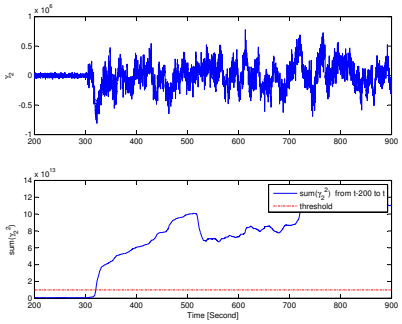

Fig. 9. Upper subplot shows the comparison output γ_2 of the sensors at the second blades while sensor S_2^1 has a a 1.5 times its normal gain. The lower subplot shows the mean value change detection estimate from energy detector, where the dashed line is the threshold.

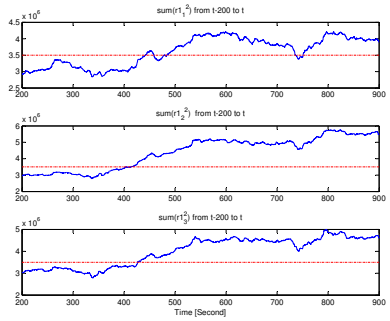

Fig. 10. Variance change detection results of the three innovation outputs of Kalman filter 1 from the energy detector while sensor S_2^1 has a 1.5 times its normal gain, where the dashed line is the threshold.

REFERENCES

Chiuso, A. (2007). The role of vector autoregressive modeling in predictor based subspace identification. *Automatica* **43**(3), 1033–1048.

Gustafsson, Fredrik (2000). *Adaptive Filtering and Change Detection*. Wiley. Chichester.

Kay, Steven M. (1998). *Fundamentals of statistical signal processing: Detection Theory*. Vol. II. Prentice-Hall PTR. Upper Saddle River,New Jersey.

Mangoubi, Rami S. (1998). *Robust Estimation and Failure Detection*. Springer. London.

van Engelen, T. G. (2006). Morphological study of aeroelastic control concepts for wind turbines. Technical Report ECN-E-06-056. Energy Research Center of the Nederlands. Petten, the Nederlands.

van Engelen, T. G. and E. L. van der Hooft (2003). Individual pitch control, inventory. Technical Report ECN-E-03-138. Energy Research Center of the Nederlands. Petten, the Nederlands.

Verhaegen, Michel and Vincent Verdult (2007). *Filtering and System Identification: A Least Square Approach*. Cambridge University Press. Cambridge.